Materials Research Proceedings 41 (2024) 1860-1866 https://doi.org/10.21741/9781644903131-206

Micro-milling and micro-EDM residual stresses evaluation on post-processed 3D printed samples

HIKARU Abe[1,a], BINTI JUANIH Iman Farhana[1,b], QUARTO Mariangela[2,c], ABENI Andrea[3,d], ATTANASIO Aldo[3,e], D'URSO Gianluca[2,f], GINESTRA Paola[3,g*] and MATSUMURA Takashi[1,h]

[1]Department of Mechanical Engineering, Tokyo Denki University,5 Senjyu Asahi-cho, Adachi-ku, Tokyo,120-8551, Japan

[2]Department of Management, Information and Production Engineering, University of Bergamo, Via Pasubio 7/b,24044, Dalmine, Italy

[3]Department of Mechanical and Industrial Engineering, Università degli Studi di Brescia, Via Branze 38,25123 Italy

[a]22kmk03@ms.dendai.ac.jp, [b]23kmk03@ms.dendai.ac.jp, [c]mariangela.quarto@unibg.it, [d]andrea.abeni@unibs.it, [e]aldo.attanasio@unibs.it, [f]gianluca.durso@unibg.it, [g]paola.ginestra@unibs.it, [h]tmatsumu@cck.dendai.ac.jp

Keywords: Micro Milling, Micro-EDM, Residual Stress, 3D Printed Metals

Abstract. Micromachining is essential for producing microscopic components or obtaining complicated details in high-precision devices. Micromachining on 3D-printed metal samples is a cutting-edge, interdisciplinary field that blends additive manufacturing with accurate subtractive machining processes at the microscale. This method aims to precisely remove material from 3D-Printed metal items to obtain complicated geometries with strict tolerances, and high-end surface finishes. The surface integrity is not only determined by the surface roughness, but it depends also on the residual stresses caused by the thermo-mechanical loads during the Additive Manufacturing and the Micromachining processes. This paper aims to analyze the residual stresses measurements after Micromachining with both Micro-Milling and Micro-Electrical Discharge Machining of 3D-Printed metal samples. 17-4 PH stainless steel 3D printed samples were produced with Laser Powder Bed Fusion. The analysis of the residual stresses was carried out by producing microchannels of different sizes (200 μm and 800 μm) to also investigate the scale effect.

Introduction

Micro machining of 3D printed metals represents a critical issue in the context of precision manufacturing, allowing the fabrication of precise components at microscopic scales. This process involves the use of specialized machining techniques to finish, shape, or modify Additive manufacturing (AM) metal parts with utmost precision and accuracy. The advent of 3D printing technologies has revolutionised manufacturing by enabling the creation of complex geometries that were previously challenging or impossible to produce using conventional machining methods. However, despite the complexity and precision achievable through AM, the printed components often require further finishing operations and customization, specifically in industries such as aerospace, medical devices, or electronics, where micron-level accuracy is the target. Micromachining techniques encompass a range of processes to operate at extremely high resolutions. These processes are used to achieve complex features, precise surface finishes, and tight tolerances on 3D printed metal parts. The challenge in Micromachining lies not only in the small-scale operations but also in addressing the inherent characteristics of 3D printed metals. Residual stresses, anisotropic properties, and surface roughness resulting from the AM process can influence the machinability of these materials [1], requiring specialized strategies and tooling. In

addition to conventional subtractive methods, such as Micro-Milling, non-traditional Micromachining approaches like laser machining, electrochemical machining, or Micro-Electrical Discharge Machining are also employed to achieve high precision on complex geometries and high surface finishing without introducing excessive mechanical stress [2].

Residual stresses in 3D printed metals represent internal stresses within a material that remain after the manufacturing process. They emerge due to elastic and plastic strain, thermal gradients, solidification, and phase transformations inherent in the AM process. When metals are 3D printed, each layer is sequentially deposited and rapidly cooled, causing uneven thermal contraction and solidification. This non-uniform cooling leads to localized contractions, creating internal stresses within the material. Additionally, the repeated heating and cooling cycles during the printing process can induce phase transformations, further contributing to residual stresses. These residual stresses can significantly impact the properties and performance of 3D printed components. They might cause warping, cracking, or distortion in the printed parts, reducing their structural integrity and dimensional accuracy. Moreover, residual stress tends to be compressive near the center of part and tensile near the surfaces [3]. In fact, compressive residual stresses can play a beneficial role in reinforcing the longevity and durability of components, particularly in metallurgy and manufacturing [4]. The evaluation and management of residual stresses in 3D printed metals are critical to ensure the reliability and quality of the final products. Various techniques, such as simulation methods, X-ray diffraction, neutron diffraction, and strain gauge methods, are employed to measure and understand these internal stresses [5]. Mitigation strategies, including post-processing treatments like heat annealing, are often implemented to reduce residual stresses and enhance the overall performance and durability of 3D printed metal components.

The evaluation of residual stresses on 3D printed metals processed by Micromachining techniques [6] can be crucial both for the final application and for the understanding of the micro mechanisms that occur during the material removal process [7] on metals produced by AM. This paper aims to evaluate Residual Stresses (RS) on machined samples produced by Laser Powder Bed Fusion (LPBF). The samples have been machined with Micro-Milling (MM) and Micro-Electrical Discharge Machining (micro-EDM) and the residual stresses have been analysed on processed samples.

Materials and Methods

Additive Manufacturing: The AM samples had a square base measuring 25 x 25 mm and a height of 2.2 mm, designed as parallelepipeds. For the LPBF process, in order to prevent contaminants, the samples were produced in a Nitrogen atmosphere with a regulated O_2 level of less than 0.1 vol.%, using the commercial LPBF machine ProX 100 (3D System, Rock Hill, USA). The parameters of LPBF were: laser power of 100W, scan speed of 300 mm/s, and layer thickness of 30 µm. 17-4 PH stainless steel (3D Systems, USA) powder has been used for the production and the samples have been machined as-built, without heat treatment.

Micro-machining (MM): The MM tests were performed on the ultra-precision five-axis nano-precision machining center KERN Pyramid Nano (Kern Micro Technik, Olympiastr. 2, D-82418 Murnau-Westried, Germany) with a spindle able to reach 50000 RPM, equipped with a Heidenhain iTCN 530 numeric control. The microfeatures were machined by tungsten carbide tools with titanium nitride coating with a nominal diameter of 200 µm (RIME HM79/02) and 800 µm (RIME HM79/02). Microchannels of 200 µm and 800 µm width and a constant length of 5 mm were machined in a single pass. The depth of the channels was 20 µm for the 200 µm channels and 50 µm for the 800 µm channels. The Material Removal Rate (MRR) was calculated as the product of the feed rate and the section of the machined channels, to compare MM with micro-EDM. With a tool diameter of 200 µm, the feed per tooth was kept at 1 µm/tooth, the cutting speed was set at 22 m/min and the MRR was 0.28 mm^3/min. With a tool diameter of 800 µm, the feed per tooth was kept at 3 µm/tooth, the cutting speed was set at 40 m/min and the MRR was 3.82 mm^3/min.

Micro-EDM: tests were performed on Sarix SX-200 micro-EDM, with CAM software to define the electrode paths. Two cylindrical tungsten carbide electrodes were chosen with 200 µm and 800 µm diameters. The current peak and width, in relation to electrode, materials, and geometry, determined the MRR. A medium pulse shape, a peak current index of 100, a voltage of 100 V, and a width of 4 µs were set for all the tests. The average value of the MRR for the 200 µm channels was 0.00169 mm^3/min while the MRR for the 800 µm channels was 0.01074 mm^3/min.

The channels were machined on four pockets, each with a depth of 0.2 mm on the top surface of the AM samples. The sample surfaces were pre-machined using a four-flute flat-bottom end mill with a nominal diameter of 3 mm. Further machining and pre-machining details are reported in [6]. The MM and micro-EDM cutting conditions have been chosen on the basis of previous analyses and researches on conventional and AM metals [1, 2, 6].

Residual stresses and FIB evaluation: The residual stresses were evaluated with a µ-X360s Residual stresses analyzer (© Pulstec Industrial Co.,Ltd, Japan). For each sample (Fig. 1), the residual stress of each point parallel to the feed direction is measured one time in four different directions (90° intervals). Table 1 reports the parameters used for the evaluation of the RS.

Table 1. Parameters used for the RS analysis with µ-X360s.

Parameter	**Value**
Collimator type	1 mm diameter
X-ray target material	Cr
X-ray tube voltage (kV)	30
X-ray tube beam current (mA)	1.0
X-ray incidence angle (°)	35
Spectra count time (s)	90 (depending on conditions)

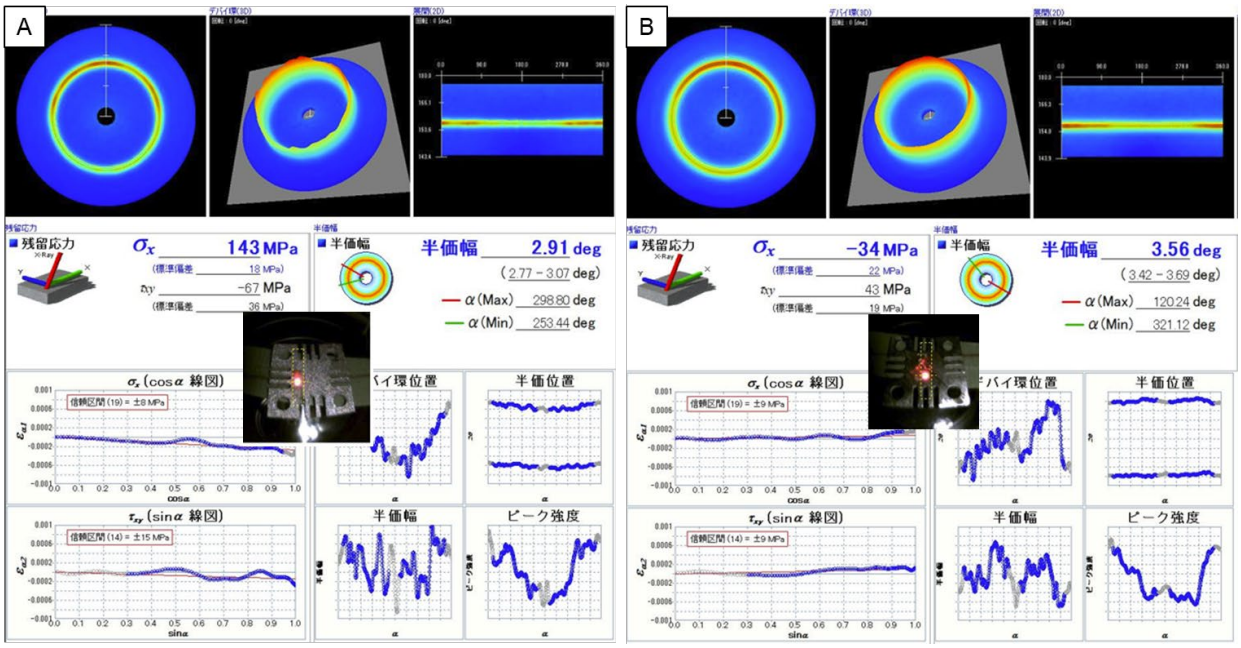

Figure 1. An example of the RS measurement at 0° degrees: EDM processed samples (A) and MM samples (B). The images shown are for illustration purposes only.

The Focused Ion Beam system used in this work to observe the samples was the Hitachi FIB-SEM system (SMI2050-D, Hitachi High Tech, Tokyo, Japan) at 30 kV. The samples are sequentially milled using an ion beam perpendicular to the specimen while imaging the exposed surface using an electron beam. This approach allows larger scale nano-structures to be

characterized by SEM. The process is destructive, since the specimen is being sequentially milled away after each image is collected. The collected series of images is then reconstructed to a 3D volume by registering the image stack and removing artifacts.

Each analysis was carried out on three replicas with three measurements repetitions.

Results

The RS measured in this study are not including only the residual stresses of the pure channel, but also part of the residual stresses around the channels, as indicated by the yellow circles in Fig. 2, which highlight the measurement area. Anyway, considering the intensity of the X-ray as a Gaussian distribution, the values of RS are estimated as that of the center of groove, due to the higher intensity of the X-ray around the center of the measured area. For reference, the maximum X-ray penetration depth in the RS measurement is about 10 μm, but the actual penetration depth is shallower due to the inclination of the device.

Regarding micro-EDM, due to the metallurgical changes and the action of high temperatures, compressive RS appears (Fig. 2). Specifically, micro-EDM is characterized by an increase of the temperature in a very localized area: the area surrounding the processed zone does not undergo this rapid increase in temperature and therefore the melted material tends to resolidify in a constrained area surrounded by lower temperatures which can generate compressive RS. Isotropic (bidirectional) residual stress is observed. That is associated with the uniform distribution of the individual discharges in micro-EDM. With the increment in the discharge energy (it corresponds to the increment of MRR), the residual stress also increases. This may be attributed to the increase in thickness of the defective white layer, in which the RS is a maximum. The RS measured for the 0.8 mm channels tends to be more tensile than the RS on the 0.2 mm channels (as shown in the example of Fig.1 A and reported in literature [8]). However, observing the 0.2 mm channels measurement area, it is worth noticing that is more influenced by the surrounding surface state that has been previously machined.

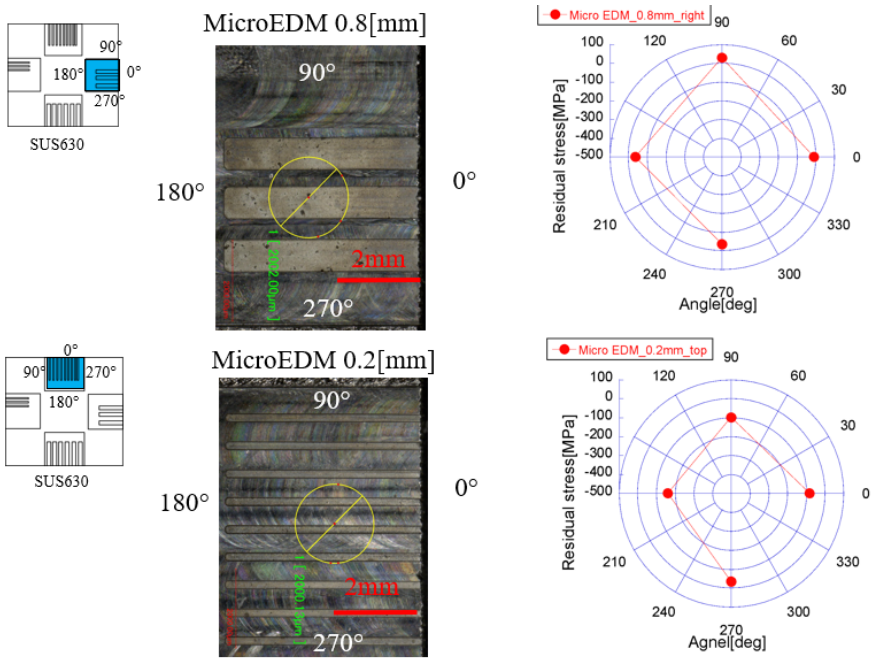

Figure 2. RS measurements at four degrees on the micro-EDM processed samples.

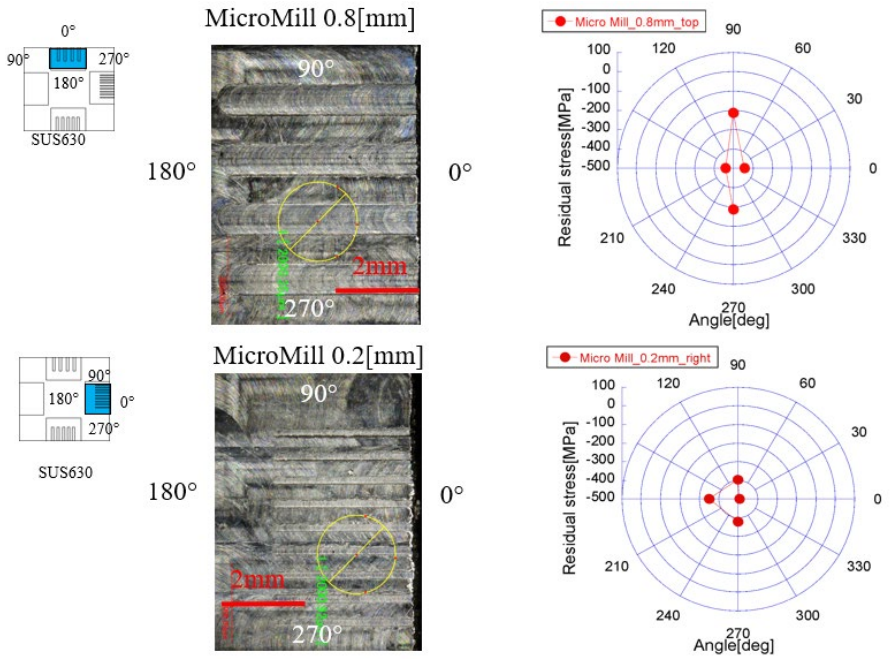

Figure 3. RS measurements at four degrees on the MM processed samples.

Regarding MM, in which the relative movement between the tool edges and the workpiece determines the chip formation, the mechanical effect highly influences the RS. Observing the results of Fig.3, the size of the tool seems to have a significant effect. Specifically, the surface machined with D0.8 mm micro tool exhibits compressive residual stress in feed direction (0°) almost two-times higher than the traversal axis direction (perpendicular to the feed direction). This effect is confirmed in literature [9] demonstrating that in conventional size milling, the RS on the machined surface in feed direction are higher than the RS along the traversal axis direction (90°). On the other hand, the surface machined with D0.2 mm micro tool shows more uniform residual stress, as visible in Fig. 3.

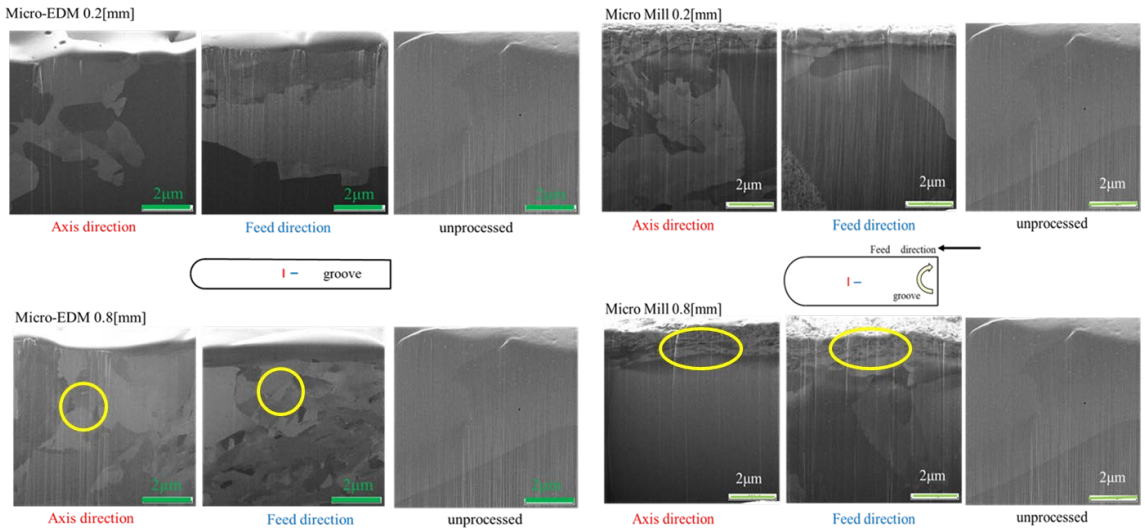

Figure 4. FIB cross section of micro-EDM and MM samples showing the differences between the tool diameters used and the measurement direction in relation to the traversal axis and feed direction. Yellow circles referring to the 0.8 mm features indicate examples of the different grain structure (micro-EDM) and white layer (MM).

Figure 4 shows the results of FIB-SEM analysis. It allows comparing the microstructure of the surface of unprocessed samples with the post-machined surfaces, both in feed and traversal axis directions. About micro-EDM sample, the larger electrode allows for observing greater thermal effects in the region immediately below the machined surface: a different grain structure is distinguishable between the two rows of images, specifically, along the feed direction. This can be related to the higher amount of energy transferred to the machined surfaces by the use of a bigger electrode which generates more sparks. Moreover, a white layer, due to the resolidified material typical of EDM processes, can be observed, with a thickness proportional to the electrode diameter. From the analysis, it is possible to exclude the presence of micro-cracks.

About MM, a superficial white layer is also visible regardless of the tool size. Its thickness appears proportional to the tool diameter. The formation of this brittle and hard white layer consisting of martensite is typical in machining of hard materials when the frictional heating is followed by the subsequent cooling process [10].

Conclusions

This work shows a preliminary analysis of the residual stresses caused by the post-processing of 3D printed metal samples with different Micromachining techniques. Considering the up-to-date literature and the related promising applications, micro-EDM and Micro-Milling have been taken into account for this analysis. It is worth remembering that tensile residual stresses are usually considered more damaging than compressive residual stresses.

- A few differences between tensile and compressive stresses can be observed and need to be highlighted. Specifically, it can be noticed that micro-EDM samples show lower compressive RS compared to the MM ones, probably due to the residual stresses caused by the LPBF technique combined with the stresses appeared during micro-EDM local melting and subsequent solidification [11].
- Micro-EDM was carried out on pre-machined samples, therefore, it would be reasonable to conclude that the typical tensile stresses on the surface of LPBF parts have been balanced with compressive stresses introduced by the pre-machining step and subsequently, further tensile stresses have been caused by micro-EDM.
- MM induced stresses, are purely compressive and dependent on the feed direction. Moreover, the compressive MM stresses seem dependent on the tool size. In MM, a tensile state of pre-stress can be detrimental in terms of burr formation and the occurrence of the ploughing phenomenon [12].

These results can be further analysed to understand which type of post-processing treatments are necessary for 3D printed metals, especially in the case of laser-powder bed fusion parts. Moreover, the analysis of residual stresses, especially on the surface, can support the mechanical characterization of machined 3D structures for bespoke and load bearing applications. Furthermore, different 3D printing techniques can cause severe and diverse residual stresses on metal samples, highlighting the need for residual stresses evaluation on as-built, treated, and machined parts.

Funding

Financed by the European Union - NextGenerationEU (National Sustainable Mobility Center CN00000023, Italian Ministry of University and Research Decree n. 1033 - 17/06/2022, Spoke 11 - Innovative Materials & Lightweighting - CUP: D83C22000690001). The opinions expressed are those of the authors only and should not be considered as representative of the European Union or the European Commission's official position. Neither the European Union nor the European Commission can be held responsible for them.

References

[1] A., Abeni, P.S., Ginestra, A. Attanasio. Micro-milling of Selective Laser Melted Stainless Steel. In: Ceretti, E., Tolio, T. (eds) Selected Topics in Manufacturing. Lecture Notes in Mechanical Engineering. (2021) Springer, Cham. https://doi.org/10.1007/978-3-030-57729-2_1

[2] M., Quarto, G. Maccarini. Surface Quality Improvement Techniques for 3D Printed Metal Samples. In: Carrino, L., Galantucci, L.M., Settineri, L. (eds) Selected Topics in Manufacturing. Lecture Notes in Mechanical Engineering. (2024) Springer, Cham. https://doi.org/10.1007/978-3-031-41163-2_3

[3] C. Li, Z.Y. Liu, X.Y. Fang, Y.B. Guo, Residual Stress in Metal Additive Manufacturing, Procedia CIRP, Volume 71, (2018) Pages 348-353, ISSN 2212-8271, https://doi.org/10.1016/j.procir.2018.05.039

[4] E.S.; Statnik, F.; Uzun, S.A.; Lipovskikh, Y.V.; Kan, S.I.; Eleonsky, V.S.; Pisarev, P.A.; Somov, A.I.; Salimon, Y.V.; Malakhova, A.G.; Seferyan, et al. Comparative Multi-Modal, Multi-Scale Residual Stress Evaluation in SLM 3D-Printed Al-Si-Mg Alloy (RS-300) Parts. Metals (2021) 11, 2064. https://doi.org/10.3390/met11122064

[5] QP Ma, J Mesicek, F Fojtik, J Hajnys, P Krpec, M Pagac, J Petru. Residual Stress Build-Up in Aluminum Parts Fabricated with SLM Technology Using the Bridge Curvature Method. Materials (Basel). (2022) Sep 1;15(17):6057. doi: 10.3390/ma15176057. PMID: 36079438; PMCID: PMC9457910

[6] A., Abeni, M. Quarto, & P.S Ginestra. Post-processing of powder bed fused stainless steel: micro-machining and micro-electrical discharge machining. J Intell Manuf (2023). https://doi.org/10.1007/s10845-023-02277-z

[7] S. Tamura, A. Ezura, and T. Matsumura, “Cutting Force in Peripheral Milling of Additively Manufactured Maraging Steel,” Int. J. Automation Technol., (2022) Vol.16 No.6, pp. 897-905,

[8] S. Schneider, J. Vorspohl, F. Frerichs, A. Klink, M. Meinke, W. Schröder, T. Lübben, Investigation on residual stress induced by multiple EDM discharges, Procedia CIRP, Volume 102, (2021), Pages 482-487, ISSN 2212-8271, https://doi.org/10.1016/j.procir.2021.09.082.

[9] H., Liu, D.Schraknepper , T. Bergs. Investigation of residual stresses and workpiece distortion during high-feed milling of slender stainless steel components. Procedia CIRP, 108, (2022). 495-500.

[10] S. K.,Rajbongshi, D. K., Sarma, M. A. Singh. (A Brief Review of White Layer Formation in Hard Machining with a Case Study. In Advances in Mechanical Engineering: Select Proceedings of ICRIDME (2020). pp. 407-417. Springer Singapore.

[11] R. Acevedo, P. Sedlak, R. Kolman, M. Fredel, Residual stress analysis of additive manufacturing of metallic parts using ultrasonic waves: State of the art review, Journal of Materials Research and Technology, Volume 9, Issue 4, (2020), Pages 9457-9477, ISSN 2238-7854, https://doi.org/10.1016/j.jmrt.2020.05.092

[12] R., Yadav, N.D. Chakladar, S. Paul. Effects of tailored residual stress on micro-end milling: numerical modelling and validation. Int J Adv Manuf Technol 127, 5449–5470 (2023). https://doi.org/10.1007/s00170-023-11780-9